

THE SPITZER IRS SPECTRUM OF SMP LMC 11

J. BERNARD-SALAS,¹ E. PEETERS,² G. C. SLOAN,¹ J. CAMI,² S. GUILES,¹ AND J. R. HOUCK¹

Received 2006 June 2; accepted 2006 September 8; published 2006 October 26

ABSTRACT

We present the first mid-infrared spectra of SMP LMC 11 in the Large Magellanic Cloud. While this object resembles a planetary nebula in the optical, its infrared properties are more similar to an object in transition from the asymptotic giant branch to the planetary nebula phase. A warm dust continuum dominates the infrared spectrum. The peak emission corresponds to a mean dust temperature of 330 K. The spectrum shows overlapping molecular absorption bands from 12 to 17 μm corresponding to acetylene and polyacetylenic chains and benzene. This is the first detection of C_4H_2 , C_6H_2 , C_6H_6 , and other molecules in an extragalactic object. The infrared spectrum of SMP LMC 11 is similar in many ways to that of the preplanetary nebula AFGL 618. The IRS spectrum shows little evidence of nitrogen-based molecules that are commonly seen in Galactic asymptotic giant branch stars. Polycyclic aromatic hydrocarbons are also absent from the spectrum. The detection of the [Ne II] 12.8 μm line in the infrared and other forbidden emission lines in the optical indicates that an ionized region is present.

Subject headings: circumstellar matter — infrared: general — ISM: lines and bands — ISM: molecules — planetary nebulae: individual (SMP LMC 11) — stars: AGB and post-AGB

1. INTRODUCTION

The transition from the asymptotic giant branch (AGB) to the planetary nebula (PN) phase remains an elusive stage in stellar evolution. At the end of its lifetime on the AGB, a star loses mass at high rates, triggering the formation of molecules and dust in a thick circumstellar envelope (e.g., Habing 1996; Blommaert et al. 2005). Radiation pressure on the dust and coupling between the dust and gas drive the outflows, stripping the star and exposing its hot core. As the effective temperature of the exposed core rises, it will ionize the nebular gas.

The detailed chemistry involved in this brief transition phase is poorly understood. In carbon-rich stars, carbon is primarily incorporated first into carbon monoxide (CO) and then into acetylene (C_2H_2). Acetylene and its derivatives are the precursors from which carbon-based compounds such as polycyclic aromatic hydrocarbons (PAHs) and soot are formed (Allamandola et al. 1989; Frenklach & Feigelson 1989). Here we present the infrared spectrum of SMP LMC 11, an object in the Large Magellanic Cloud (LMC) whose infrared spectral characteristics fall in the stage where most of this complex chemistry takes place.

SMP LMC 11 was part of the Sanduleak et al. (1978) survey of PNe in the Magellanic Clouds (from which it takes its designation, SMP LMC 11). It was also included in the catalog by Leisy et al. (1997) of accurate positions of known PNe in the LMC. The reported $\text{H}\beta$ flux and extinction vary among papers in the literature. For instance, Leisy & Dennefeld (2006), Wood et al. (1987), and Meatheringham et al. (1988) report a $\log \text{H}\beta = -13.14$ (with $\text{H}\beta$ in units of $\text{ergs cm}^2 \text{s}^{-1}$), whereas Shaw et al. (2006) obtain $\log \text{H}\beta = -13.94$. Similarly, differences in visual extinction amount to a factor of more than 3. The presence of another source nearby in the IRAC images (see § 2) may explain these discrepancies. Morgan & Parker (1998) presented optical spectroscopy of 97 faint PNe including SMP LMC 11 and identified the forbidden emission lines of [O III], [N II], and [S II]. Recently, Shaw et al. (2006) observed it with the *Hubble Space*

¹ Center for Radiophysics and Space Research, Cornell University, 219 Space Sciences Building, Ithaca, NY 14853-6801; jbs@isc.astro.cornell.edu, sloan@isc.astro.cornell.edu, jrh13@cornell.edu.

² SETI Institute, 515 North Whisman Drive, Mountain View, CA 94043; epeeters@mail.arc.nasa.gov, jcami@mail.arc.nasa.gov.

Telescope (*HST*) as part of their sample of objects in the LMC and SMC. They measured the strength of the [O I] line, along with the previously identified forbidden lines, and inferred a bipolar morphology with a size of $0''.76 \times 0''.55$.

In this Letter we report the first mid-infrared spectrum of SMP LMC 11. The spectrum reveals a wealth of molecular absorption bands and a few atomic emission lines. To our knowledge, the only other object showing a similar infrared spectrum is the Galactic preplanetary nebula³ (PPN) AFGL 618. Bujarrabal et al. (1988) inferred that AFGL 618 became a PPN only 200 yr ago. Chiar et al. (1998) identified simple aliphatics (CH_2 , CH_3) in its spectrum at 3.4 μm . Cernicharo et al. (2001b) studied the spectrum of AFGL 618 from the Short Wavelength Spectrometer (SWS; de Graauw et al. 1996) on the *Infrared Space Observatory* (*ISO*; Kessler et al. 1996), and they describe the system as having a thick molecular envelope surrounding a B0 star and an ultracompact H II region. They suggest that UV radiation from the central star and shocks in the high-velocity winds have significantly modified the chemistry. Cernicharo et al. (2001b) detected C_4H_2 , C_6H_2 and of C_6H_6 in a circumstellar environment for the first time. In this Letter we compare the observed features in SMP LMC 11 to those of AFGL 618.

Section 2 describes the observations and the data reduction techniques. Section 3 gives the analysis of the observed spectral features and compares SMP LMC 11 to AFGL 618. Section 4 discusses the evolutionary status of the object.

2. OBSERVATIONS AND DATA REDUCTION

We observed SMP LMC 11 with the Infrared Spectrograph (IRS; Houck et al. 2004) on board the *Spitzer Space Telescope* (Werner et al. 2004) as part of the GTO program on 2005 June 6 (program ID 103, AOR key 4947712). These observations consist of spectra from all four IRS modules: Short-Low (SL), Long-Low (LL), Short-High (SH), and Long-High (LH). Table 1 gives the wavelength coverage, spectral resolution, and integration times for each module. We performed peak-up on a nearby star to achieve accurate pointing ($0''.4$).

³ We adopt the term “preplanetary nebula” to avoid the confusing term “protoplanetary nebula,” which could imply an object evolving into a PN or a nebula with embedded protoplanets.

TABLE 1
OBSERVATION LOG OF SMP LMC 11

Module	Order	Wavelength (μm)	Resolution	Obs. Time ^a
SL	1	7.5–14.5	60–120	14 \times 2
SL	2	5.0–7.5	60–120	14 \times 2
LL	1	20–40	60–120	30 \times 1
LL	2	14.5–20	60–120	30 \times 1
SH	11–20	10–20	600	60 \times 1
LH	11–20	20–36	600	120 \times 1

^a On-source observation time in seconds times the number of cycles.

The data were processed through a copy of the *Spitzer* Science Center's pipeline reduction software (ver. S13.2) maintained at Cornell. To avoid possible problems in the flat field, we chose to start the reduction analysis from the un-flat-fielded (droopres) images. From there, the reduction and extraction techniques were carried out as follows: Rogue pixels and flagged data were removed using the *irsclean*⁴ tool, which uses a mask of rogue pixels for each campaign to first flag and then remove rogue pixels. These rogue pixels are especially troublesome in LH. To remove the contribution from the background in the low-resolution modules (SL and LL), the images were differenced nod-nod (e.g., SL1 nod 1–SL1 nod 2). Spectra were extracted from the images using a script version of the Cornell-developed software package SMART (Higdon et al. 2004), using variable-column extraction for SL and LL, and full-slit extraction for SH and LH.

The spectrum was calibrated by dividing the extracted spectrum of the source by the extracted spectrum of a standard star (HR 6348 for SL and LL, and ξ Dra for SH and LH) and multiplying by its template (Cohen et al. 2003; G. C. Sloan 2006, in preparation). Spikes that were not present in both nod positions or in the overlap region between orders were treated as artifacts and were removed manually.

It is important to note that there is a significant mismatch between the different modules, probably due to the presence of another source about 4" from the target, which is revealed in the IRAC images from the SAGE program (Meixner et al. 2006), and which is included in the LL and LH slits. Pointing effects may also be present. We used the coordinates reported by Leisy et al. (1997), which differ from the coordinates recently reported from *HST* observations (Shaw et al. 2006) by 3" in R.A. We scaled the modules to match the average spectrum of the two nod positions in SH, because the difference between the two nods in SH is of only 5% and one of the nod positions avoids the contaminating source.

3. ANALYSIS

Figure 1 (*top*) shows the resulting low-resolution spectrum of SMP LMC 11 together with the IRAC (Infrared Array Camera; 5.8 and 8 μm), MIPS (Multiband Imaging Photometer for *Spitzer*; 24 μm), and IRAS (*Infrared Astronomical Satellite* [Beichman et al. 1988]; 25 μm) fluxes. A cool dust component dominates the overall shape of the continuum emission. The spectrum also shows broad absorption bands, most notably between 12 and 17 μm .

3.1. The Dust Continuum

The dashed line in Figure 1 (*top*) is a spline fit to the dust continuum; the gray circles indicate the anchor points. In the

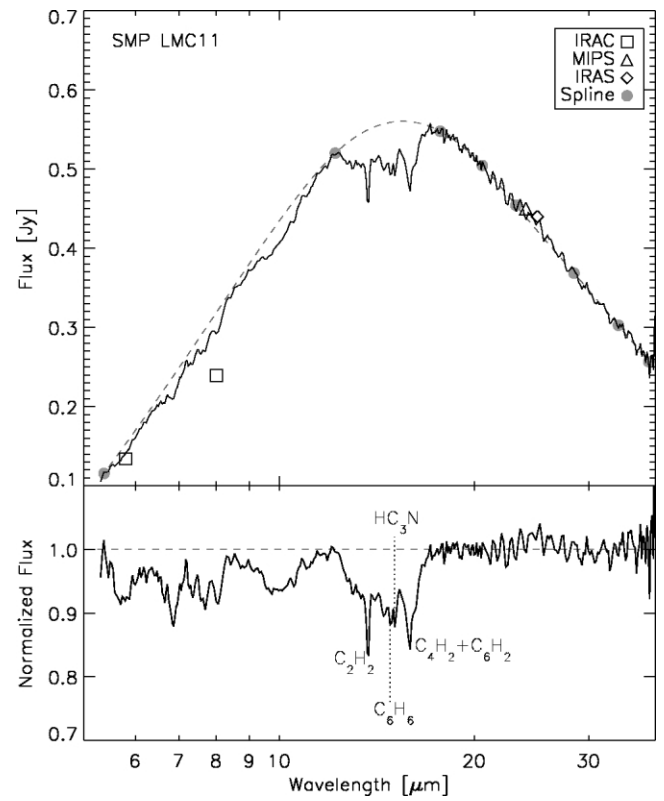


FIG. 1.—Low-resolution spectrum of SMP LMC 11 (*top*). The dashed line indicates a spline fit representing the assumed continuum. The photometric points correspond well with IRS spectrum except for the 8 μm IRAC, which is slightly lower. The bottom panel shows the continuum-divided spectrum, revealing a wealth of absorption features due to various molecules (see Fig. 2 and text for more details).

short-wavelength region we anchored to the maximum emission at only two points, 5 and 12 μm . While this is an arbitrary choice, the resulting absorption spectrum is in accordance with the lack of emission features seen in the rest of the spectrum. Given the carbon-rich nature of the gas and the lack of broad emission features in the spectrum (such as PAHs), it is reasonable to assume that amorphous carbon grains dominate the dust mixture. The dust continuum in Figure 1 is featureless and peaks at 15.5 μm , implying that the bulk of the emitting dust is at 330 K. For the remainder of this Letter, we represent the dust continuum by the spline fit shown in Figure 1.

3.2. Absorption Features

The bottom panel of Figure 1 shows the spectrum of SMP LMC 11 after dividing out the dust continuum and reveals a number of molecular bands visible even at low resolution. Similarly, Figure 2 shows the high-resolution spectrum of SMP LMC 11 and the *ISO* SWS spectrum of AFGL 618 for comparison. In Figure 2 the narrow spectral features in SMP LMC 11 are very similar to those in AFGL 618.

The high-resolution spectrum of SMP LMC 11 shows broad absorption between 12 and 17 μm with a wealth of narrow lines superposed. These are the unresolved *Q*-branches of various rovibrational bands from different molecules, many of which can be identified by comparison to AFGL 618 as due to acetylene (C_2H_2 , 13.70 μm), diacetylene (C_4H_2 , 15.87 μm), triacetylene (C_6H_2 , 16.10 μm), benzene (C_6H_6 , 14.85 μm), and HC_3N (15.10 μm). Most of these also appear in the low-resolution spectrum (Fig. 1). The strongest *Q*-branch is the one due to C_2H_2 at 13.7 μm . Close inspection of the spectrum

⁴ This tool is available from the SSC Web site: <http://ssc.spitzer.caltech.edu>.

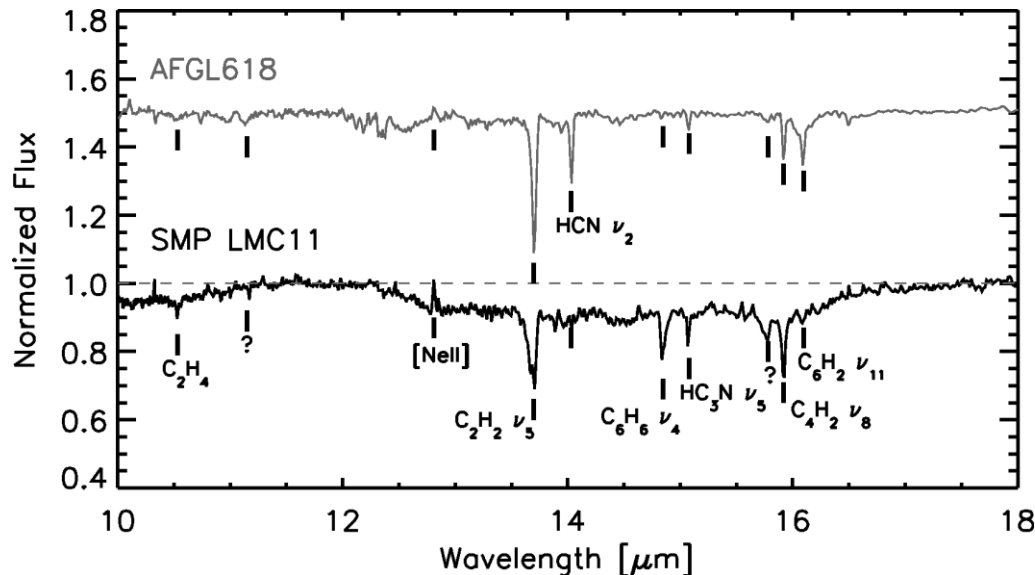


FIG. 2.—Normalized IRS high-resolution spectra (SH) of SMP LMC 11, adopting the continuum from Fig. 1 (bottom spectrum). For comparison, the normalized *ISO* SWS spectrum of AFGL 618 is also shown in gray with an offset of 0.5. The spectrum of AFGL 618 has been rebinned to the resolution of the IRS-SH module ($R \sim 600$). Many molecular bands are clearly present in both spectra, and some are only present in the spectrum of SMP LMC 11. Q -branch bands are indicated with vertical tick marks with their identification if known.

indicates the presence not only of the fundamental ν_5 mode but also of hot bands and combination bands. The broad absorption is the result of the superposition of the many P - and R -branch lines that correspond to these Q -branches, which indicates that the column densities of these species must be high. SMP LMC 11 presents a weaker triacetylene band compared to AFGL 618 but in contrast shows a stronger benzene band. Ammonia (NH₃, with the strongest bands at 10.35, 10.75, and 6.15 μm) and HCN (at 14.01 μm) are at most marginally present. By contrast, stronger rovibrational bands of HCN are present in AFGL 618 and in the extreme carbon star IRC +10 216 (Cernicharo et al. 1999). Figure 1 shows that the spectrum also exhibits an absorption dip near 10 μm . Such a dip is also seen by Zijlstra et al. (2006) in their sample of carbon stars. They attribute this feature to C₃; however, this identification is still a matter of debate (e.g., Speck et al. 2006).

The spectrum of SMP LMC 11 shows features that are not seen in AFGL 618 at 10.53, 11.15, and 15.78 μm . The feature at 10.53 μm corresponds to the Q -branch of the ν_7 CH₂-wagging mode of C₂H₄ (ethylene). In the *Spitzer* wavelength range, the only other mode of this molecule that would be expected is the strong scissoring mode at 6.93 μm ; the rocking mode at 12.10 μm is expected to be weak. There is indeed a feature around 6.93 μm in the low-resolution spectrum (Fig. 1). CH₃C₂H, also known as propyne or methylacetylene, has its strongest band at 15.79 μm with medium-strength bands at 6.84 and 7.97 μm , and the spectrum of SMP LMC 11 shows bands at both of those wavelengths (see Fig. 1). Therefore, propyne may be a good candidate for the 15.78 μm band. However, the absorption from 6.3 to 8.3 μm in Figure 1 (bottom panel) can also be due to the C₂H₂ $\nu_4 + \nu_5$ bands, which have been identified by Matsuura et al. (2006) in a sample of LMC AGB stars. With the latter identification, the 8.0 μm feature could be ascribed to the C₄H₂ $\nu_6 + \nu_8$ band. The blue shoulder of this band in our spectrum may be due to HCN. Sloan et al. (2006) noted that the two absorption bands from C₂H₂ at 7.5 and 13.7 μm are decoupled in their sample of carbon stars in the SMC. Thus, we cannot use the lack of a 14.0 μm band from HCN to rule out a contribution of HCN at 7.1 μm . CH₃

at 7.2 μm and CH₄ at 7.7 μm have been seen in AFGL 618 (Cernicharo et al. 2001a) and in Titan's atmosphere (Coudé du Foresto et al. 2003), and they could also be contributing to this band in SMP LMC 11. A firm identification of these bands will require higher resolution observations, especially from the ground and the *James Webb Space Telescope*, complemented with a detailed comparison with laboratory measurements. Besides the absorption features mentioned above, the spectrum of SMP LMC 11 shows no traces of the MgS feature ($\sim 30 \mu\text{m}$) that is commonly seen in carbon stars with optically thick dust shells and on some PNe.

3.3. Emission Lines

In addition to the absorption features, the high-resolution spectrum of SMP LMC 11 clearly shows emission from [Ne II] at 12.8 μm . The [Ne III] line (15.5 μm) may be present, but the presence of another line at 15.65 μm which may be a glitch makes the identification of the [Ne III] more doubtful. The presence of the low-excitation line of [Ne II] is consistent with the optical measurements by Morgan & Parker (1998) and Shaw et al. (2006) of the low-excitation lines of [N II], [S II], [O I], and [O III].

4. DISCUSSION

The infrared spectrum of SMP LMC 11 reveals three components: a cool dust continuum, absorption bands from hydrocarbon molecules, and emission from at least one low-ionization forbidden line.

The mean temperature of the dust as inferred from the peak of the IR emission (~ 330 K) falls closer to the most evolved AGB stars ($T \gtrsim 300$ K) than the youngest PNe ($T \sim 150$ K) (Kwok 2000). The peak of the dust emission will shift to longer wavelengths as dust moves farther away from the central star.

The *Spitzer* spectrum of SMP LMC 11 represents the first extragalactic detection of several molecules, including diacetylene (C₄H₂), triacetylene (C₄H₂), benzene (C₆H₆), HCN, C₂H₄, and possibly propyne. These molecules are the building blocks from which more complex hydrocarbons are produced (Cernicharo et al. 2001b). The absorption bands are due to the increase in thickness of the circumstellar shell, which is more dramatic

at the very end of the AGB phase (García-Lario & Perea Calderón 2002). For free molecules, this absorption will not be a Gaussian or a Lorentzian but will be a complex addition of many individual rovibrational lines with different strengths (which depend on the temperature), causing the strong absorption we see in the 12–17 μm region (due to the *P*- and *R*-branches of the molecules present in that region). The stronger absorption in this region compared to AFGL 618 indicates that SMP LMC 11 has a larger molecular column density.

The spectrum of SMP LMC 11 does not contain any PAH emission features. A mixture of PAHs and the PAH-precursor C₂H₂ are seen together in the low-resolution IRS spectrum of the post-AGB object MSX SMC 029 (Kraemer et al. 2006). The absence of PAH emission in SMP LMC 11 can be attributed to age or orientation effects. Cernicharo et al. (2001b) propose that PAHs may not form until the end of the AGB phase, based on their observations of AFGL 618. Alternatively, the dust in SMP LMC 11 could be distributed in an edge-on torus while MSX SMC 029 is seen more pole-on or has a more spherically symmetric dust distribution. The PAHs emit in photodissociation regions, and in an edge-on torus, we would not have a clear line of sight to the emitting region. The dust envelope is still too thick to allow a direct line of sight into the hotter central regions.

Despite the detection of HC₃N (and perhaps HC₅N), the spectrum of SMP LMC 11 shows evidence for reduced abundances of nitrogen-based molecules such as HCN and NH₃ compared to Galactic objects like AFGL 618. This agrees with the nitrogen abundance derived by Leisy & Dennefeld (2006) for SMP LMC 11 [log (N/H) + 12 = 7.1], which is one of the lowest in their sample of LMC PNe. This result fits with the finding of Matsuura et al. (2006) that the HCN bands that are prominent in the Galactic sample of carbon stars are significantly weaker or absent in the LMC sample. The lower nitrogen abundance in the LMC compared to the Galaxy and higher efficiency of the third dredge-up at lower metallicities work together to decrease the nitrogen abundance relative to carbon.

The presence of an optically thick and relatively warm dust component between us and the central ionized region can explain not only the absence of PAH features but also the absence of most

ionized lines in the infrared. We only see [Ne II] (and maybe [Ne III]), and this line is probably visible only in scattered light. Scattering is more efficient in the optical than in the infrared, which would explain why more of the forbidden lines can be detected in the optical. The dust also explains the presence of molecular absorption in the spectrum, since the molecules do not have a direct line of sight to the still-shielded central ionized region. It is also possible that some of the forbidden line emission is excited by high-velocity ($v > 100 \text{ km s}^{-1}$) shocks (Leisy & Dennefeld 2006). All of these properties are more consistent with an object that is in transition from the AGB to a PN than with a classic PN.

The bright H β luminosity and its large size present some problems with this scenario of a transition object. While the measured H β flux by Shaw et al. (2006) makes SMP LMC 11 one of the faintest PNe in their LMC sample, its equivalent flux at 1 kpc (if we assume that it is at a distance of 50 kpc) is $\log H\beta = -10.55$, which is bright for Galactic standards. Similarly, Shaw et al. (2006) state that it is one of the smallest bipolar nebulae in their LMC sample, but at a Galactic distance of 1 kpc it would be resolved. These characteristics resemble those of a typical PN. One could then invoke a massive molecular envelope surrounding the ionized region to explain the absorption features. Still, the absence of PAHs and H₂ in the spectrum and the high temperature of the dust (compared to PNe) would remain unexplained (unless perhaps invoking a complex geometry).

The rich chemistry seen in the IRS spectrum of SMP LMC 11 makes it (together with AFGL 618, and MSX SMC 029) a key object in our understanding of the formation of hydrocarbons, deserving future study from the community. Particularly, CO measurements of the circumstellar AGB envelope may prove to be particularly useful.

We would like to thank Richard Shaw for sharing his results prior to publication, and the referee, whose diligence led to substantial improvements in the manuscript. This work is based on observations made with the *Spitzer Space Telescope*, which is operated by the Jet Propulsion Laboratory, California Institute of Technology under NASA contract 1407. Support for this work was provided by NASA through contract 1257184 issued by JPL/Caltech.

REFERENCES

Allamandola, L. J., Tielens, A. G. G. M., & Barker, J. R. 1989, ApJS, 71, 733
 Beichman, C. A., Neugebauer, G., Harbig, H. J., Clegg, P. E., & Chester, T. J. 1988, *Infrared Astronomical Satellite (IRAS) Catalogs and Atlases*, Vol. 1: Explanatory Supplement (NASA RP-1990; Washington, DC: GPO)
 Blommaert, J., Cami, J., Szczerba, R., & Barlow, M. J. 2005, Space Sci. Rev., 119, 215
 Bujarrabal, V., Gómez-González, J., Bachiller, R., & Martín-Pintado, J. 1988, A&A, 204, 242
 Cernicharo, J., Heras, A. M., Pardo, J. R., Tielens, A. G. G. M., Guélin, M., Dartois, E., Neri, R., & Waters, L. B. F. M. 2001a, ApJ, 546, L127
 Cernicharo, J., Heras, A. M., Tielens, A. G. G. M., Guélin, M., Dartois, E., Neri, R., & Waters, L. B. F. M. 2001b, ApJ, 546, L123
 Cernicharo, J., Yamamura, I., González-Alonso, E., de Jong, T., Heras, A., Escribano, R., & Ortigoso, J. 1999, ApJ, 526, L41
 Chiar, J. E., Pendleton, Y. J., Geballe, T. R., & Tielens, A. G. G. M. 1998, ApJ, 507, 281
 Cohen, M., Megeath, T. G., Hammersley, P. L., Martin-Luis, F., & Stauffer, J. 2003, AJ, 125, 2645
 Coustenis, A., Salama, A., Schulz, B., Ott, S., Lellouch, E., Encenaz, T. H., Gautier, D., & Feuchtgruber, H. 2003, Icarus, 161, 383
 de Graauw, T., et al. 1996, A&A, 315, L49
 Frenklach, M., & Feigelson, E. D. 1989, ApJ, 341, 372
 García-Lario, G., & Perea Calderón, J. V. 2002, in Exploiting the *ISO* Data Archive: Infrared Astronomy in the Internet Age, ed. C. Gry et al. (ESA SP-511; Noordwijk: ESA), 97
 Habing, H. J. 1996, A&A Rev., 7, 97
 Higdon, S. J. U., et al. 2004, PASP, 116, 975
 Houck, J. R., et al. 2004, ApJS, 154, 18
 Kessler, M. F., et al. 1996, A&A, 315, L27
 Kraemer, K. E., Sloan, G. C., Bernard-Salas, J., Price, S. D., Egan, M. P., & Wood, P. R. 2006, ApJ, 652, L000
 Kwok, S. 2000, *The Origin and Evolution of Planetary Nebulae* (Cambridge: Cambridge Univ. Press)
 Leisy, P., & Dennefeld, M. 2006, A&A, in press
 Leisy, P., Dennefeld, M., Alard, C., & Guibert, J. 1997, A&AS, 121, 407
 Matsuura, M., et al. 2006, MNRAS, 371, 415
 Meatheringham, S. J., Dopita, M. A., & Morgan, D. H. 1988, ApJ, 329, 166
 Meixner, M., et al. 2006, AJ, in press
 Morgan, D. H., & Parker, Q. A. 1998, MNRAS, 296, 921
 Sanduleak, N., MacConel, D. J., & Davis Philip, A. G. 1978, PASP, 90, 621
 Shaw, R. A., Stanghellini, L., Villaver, E., & Mutchler, M. 2006, ApJ, submitted
 Sloan, G. C., et al. 2006, ApJ, 645, 1118
 Speck, A. K., et al. 2006, ApJ, in press
 Werner, M., et al. 2004, ApJS, 154, 1
 Wood, P. R., Meatheringham, S. J., Dopita, M. A., & Morgan, D. H. 1987, ApJ, 320, 178
 Zijlstra, A. A., et al. 2006, MNRAS, 370, 1961